Sai Vinitha.G, et. al. International Journal of Engineering Research and Applications
www.ijera.com
ISSN: 2248-9622, Vol. 13, Issue 3, March 2023, pp. 51-60

RESEARCH ARTICLE OPEN ACCESS

ANFIS based Grid-connected hybrid Microgrids using Modified UIPC for power flow control

Sai Vinitha.G*, Grace Mani.K*, Praveen Kumar.Ch*, Nagabhushanam.N*, Siva Lakshmi.M*, Kiran Kumar.K**

**(UG scholar, Department of Electrical and electronics engineering, Sree Vahini Institute of Science and Technology, Tiruvuru.)*

***(HOD, Dept of Electrical and Electronics Engineering, Sree Vahini Institute of Science and Technology, Tiruvuru)*

Date of Submission: 06-03-2023 Date of acceptance: 19-03-2023

ABSTRACT

In this research, a novel method for unified interphase power controller modification-based power flow control of grid-connected hybrid microgrids with linked AC-DC microgrids is presented (UIPC). A typical grid-connected hybrid microgrid with one AC and one DC microgrid is taken into account while analyzing a system. These microgrids are integrated using a modified UIPC rather than parallel-connected power converters. The typical UIPC structure, which employs three power converters in each phase, is changed as the first contribution of this study in order to provide power exchange control across AC-DC microgrids using a smaller number of power converters. The modified structure has a power converter for each phase, known as a line power converter (LPC), and a bus power converter (BPC), which controls the DC bus voltage. The AC microgrid can operate in either capacitance mode (CM) or inductance mode and is linked to the main grid via LPCs with linked DC buses (IM). The LPCs' control mechanism uses a fuzzy logic controller and adaptive neuro fuzzy logic controllers. The H ∞ filtering approach is used to optimize the fuzzy inference system and decrease design flaws in membership functions. The DC microgrid supplies the LPCs' DC voltage via the BPC. Nevertheless, because a PV system here supplies the DC microgrid voltage, the DC link voltage of the LPCs fluctuates. Hence, a new nonlinear disturbance observer-based robust multiple-surface sliding mode control (NDO-MS-SMC) technique is provided for DC-side control of the BPC as the second contribution to stabilizing the DC link fluctuations. The simulation findings validate the efficacy of the upgraded UIPC's suggested power flow control approach for hybrid microgrids. This presents an innovative method for power flow regulation on linked AC-DC microgrids. Power exchange control between AC-DC microgrids is implemented using a modified unified interphase power controller (UIPC) for power quality improvement that is ANFIS (adaptive neuro fuzzy) controlled and employs two power converters instead of three in each phase. One power converter is included in each phase of the updated structure, and a power converter that controls the DC bus voltage is included as well and is referred to as the bus power converter (BPC). The LPCs' control mechanism uses an adaptive fuzzy logic controller. The outcomes of the MATLAB simulation support the usefulness of the upgraded UIPC's suggested power flow control method for hybrid microgrids

Keywords **-** Hybrid microgrid, UIPC, power control, disturbance observer, multi-surface SMC.

With DC microgrids, DC power resources including photovoltaic (PV), fuel cell, and energy storage systems (ESS) as well as recently introduced DC loads like programmable DC electronic loads have infiltrated the conventional power grids during the past 10 years [30]. On the other side, AC microgrids may be used to connect AC power sources like wind turbines and others to the power networks, as well as AC loads like electrical motors and others [31]. Future smart grids will incorporate AC and DC microgrids, as well as AC and DC power resources and loads, to create hybrid microgrids. Actually, the power converters are what connect the AC and DC microgrids. The microgrids can exchange power as necessary according to this connectivity. For greater power transactions and higher efficiency, the power converters are typically connected in parallel.

The general layout of a hybrid grid-connected microgrid is depicted in Fig. The DC microgrid in this diagram may consist of PV

systems, ESSs, and related loads that are linked to a shared DC bus [32]. The wind turbine, diesel generator, and AC loads connected to a single AC bus may all be included in the AC microgrid [26]. The entire hybrid microgrid can be either isolated or linked to a power system [27].

The common buses (links) of two microgrids are connected using parallel-c36635onnected bidirectional connections, as shown in Fig 1. Paralleling power converters in hybrid microgrids can provide several operational difficulties, as listed below [27-16]: The microgrids differ in terms of their dynamic properties, including voltage levels, phase, frequency, and power fluctuation. Many microgrids might be part of a hybrid microgrid. As an illustration, two AC and one DC microgrid Since the voltage magnitude and phase of the common buses of the microgrids must resemble in order to prevent current from flowing between parallel-connected ILCs, using parallel-connected ILCs to exchange power between microgrids in such a configuration with different dynamics are challenging and complicated. - Parallel-connected ILCs with equal power ratings must receive an equal amount of the power delivered across microgrids. Changes in the system parameters have an impact on the power-sharing performance of the parallel-connected ILCs.

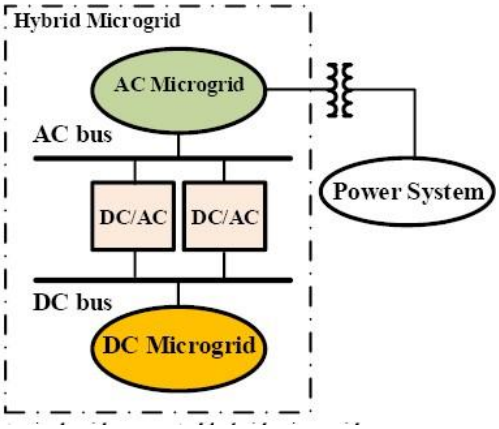

Fig 1. Grid connected hybrid microgrid

The current passing through the power converters in this case is estimated to exceed the nominal current limitations of the converters, and as a result, it may be separated, significantly reducing the power being exchanged. This might then lead to instability or even load shading in a microgrid. Many uncertainties in the power generated and oscillations in the power transferred across microgrids are brought on by some distributed generation (DG) units in microgrids that exhibit inconsistent behavior. Phase differences between ILCs as a result of harmonic distortions in AC microgrids lead to voltage loss [15]. The ILCs linked in parallel may function at various power factors. This leads to fluctuations in voltage and power and impairs the efficiency of power sharing.

Many methods and control mechanisms have been introduced into the literature to solve those challenges. For parallel-connected bidirectional ILCs, a hierarchical control technique has been brought out in [9]. The control method's platform was created in a stationary reference frame (SRF) without the use of mutual terms among the axes and with harmonic rectification. This strategy's benefit is that it is simple to implement because it was developed in the SRF. A droop control-based hierarchical control technique using a droop scheme at the first control level has been suggested in [14].

Although proportional-resonant (PR) controllers were employed on the AC side, proportional-integral (PI) controllers were employed on the DC side. The ripple that had been created as a result of the first level of control action was adjusted by the second level of control, and the utilities and hybrid microgrid were connected using the third level of control. For grid-connected hybrid microgrids, a fault-protected active power control method has been described in [7]. The approach has been used to change the strength of oscillations in active and reactive power using an adjustable scalar. Power fluctuations are a result of voltage instability, according to the authors in [15].

There was a proposed control method for ILCs that are connected in parallel that optimizes the total of the currents flowing through each power converter. Due to its higher ratings, one of the ILCs has been designated "redundant" in this regard. The control system becomes expensive as a result. Also, the approach is unable to minimize the variations in reactive power and is ineffective against harmonic distortion. A reliable control strategy for power sharing control between two parallel-connected inverters has been developed in [20]. The technique uses synthesis analysis to create the current inverter controller.

An appropriate fractional order controller for power sharing with two parallel-connected inverters has been developed in [16]. The researchers in [21] have developed structures for hybrid microgrids. For isolated microgrids, a distributed and self-optimizing control system has been developed in [12]. The local control actions offered by the control technique without any

transmission linkages significantly improved the accuracy of the method. Voltage regulation in AC transmission networks has also been modulated using Flexible AC Transmission System (FACTS) devices.

In the current research, the principle of using UIPC to manage the power shared between microgrids and the main grid in a hybrid microgrid is introduced. Many power control applications using various control topologies have employed FACTS devices. To boost voltage stability, the unified power flow controller (UPFC) has been implemented [17]. Moreover, a genetic approach has been used to select the best distribution of UPFCs. For the best possible regulation of the transmitted power in a transmission line, the inter-line power flow controller (IPFC) has been implemented [18].

In a hybrid microgrid context, this study focuses on using a simple modified UIPC to regulate the power transmitted between microgrids as well as the utility grid. This work's key contributions are as follows:
In order to govern the exchange of power between microgrids and the main grid in a hybrid microgrid, the UIPC is considered a substitute for parallel-connected power converters, which have numerous control issues [8–17]. Power exchange control across AC-DC microgrids is achieved using fewer power converters than the typical UIPC design, which calls for three power converters in each phase.

In this study, a new NDO-MS-SMC-based control approach is proposed for the DC side control of the BPC. This is because the dynamics of a hybrid microgrid are different from those of a traditional power system, making it challenging to manage the UIPC when a DC microgrid is linked to its DC bus. In order to govern load demand across various microgrids in hybrid microgrids, this study emphasized the use of the UIPC as a substitute option. The following benefits of the UIPC are above those of typical parallel-connected power converters:

Regulation of electricity shared across microgrids without imposing onerous restrictions, such as those usually needed to link the ILCs in parallel, including equivalent voltage magnitudes, phases, etc. According to [24], the UIPC can restrict the fault current with simplicity without using a redundant power converter, as detailed in [15]. This characteristic facilitates the connection. Compared to other control schemes, such as the instantaneous power control strategy, which has historically been employed for parallel-connected ILCs, it is less complex, less costly, and more dependable. The proposed modified UIPC offers a voltage isolation feature as shown in [24], even though parallel-connected ILCs offer direct electrical connections between microgrids. Both the DC bus voltage and the AC bus voltage of the AC microgrid may be controlled by the UIPC. It was not possible to provide this characteristic by using the typical parallel-connected ILCs.

The applications of the adaptive network are rapid and extensive across many fields, thanks to these few limits. We suggest a type of adaptive network in this section that is functionally comparable to fuzzy inference systems. The acronym ANFIS, which stands for "adaptive network-based fuzzy inference system, refers to the suggested design. We explain how to break down the parameter set so that the hybrid learning rule may be applied. Moreover, we show how to use simplified fuzzy if-then rules to apply the Stone-Weierstrass theorem to ANFIS and how the radial basis function network relates to this form of simplified ANFIS.

II. PROPOSED HYBRID MICROGRID AND DYNAMIC MODELING STRUCTURE BASED ON THE UIPC

This section describes the proposed hybrid microgrid topology focused on the UIPC. The dynamic model of the modified UIPC is also presented in this section. The hybrid microgrid under study is depicted in Fig. 2. The grid-connected hybrid microgrid, as mentioned, consists of two microgrids: one AC and one DC, connected by the UIPC. An AC microgrid is made up of connected AC and DC loads and a diesel generator. A PV system, a battery, and AC and DC loads exist in the DC microgrid. The loads, the PV system, and the battery are connected to the common DC bus (DC link).

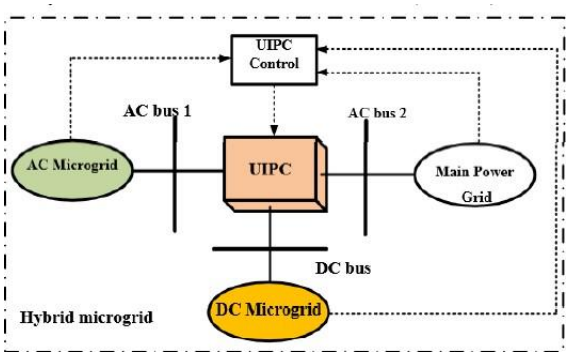

Fig.2 Interconnection of AC-DC Microgrids in Grid connected hybrid microgrid using UIPC

A. Traditional UIPC

The UIPC's per-phase model has been discussed in [24] and is shown in Fig. 3. Voltage source converters had been installed in this structure to replace the phase-shifting transformers of the interphase power controller (IPC) (VSCs). In each phase, three VSCs (VSC1, VSC2, and VSC3) link two AC buses (V1 and V2) to each other. The sequence converters VSC1 and VSC2 and voltage-regulating converter VSC3 are each used. Transformer T1 is used by VSC1 to introduce the series voltage V_{se}^{L} to the line while it is operating inductively. Transformer T2 is used by VSC2 to inject the series voltage V_{se}^{C} to the line while it is operating in capacitive mode. One of the AC outlets is connected to the third VSC or VSC3.

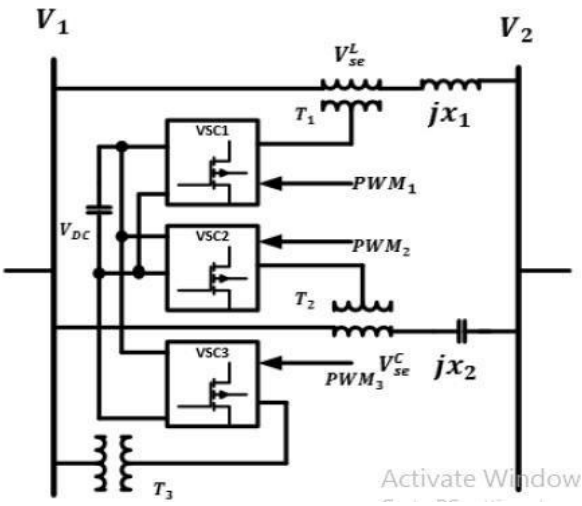

Fig.3 Conventional structure of UIPC; each phase implements three power converters [24]

Transformer T2 is used by VSC2 to inject the series voltage V_{se}^{C} to the line while it is operating in capacitive mode. The third VSC, or VSC3, controls the AC voltage and is coupled to one of the AC buses, in this case, V1, through transformer T3. All of the VSCs' DC buses are linked in parallel and are powered by a constant capacitor. Hence, each VSC's operating power is supplied by the DC link voltage or VDC.

Consequently, the transferred power between the two AC buses would be regulated by VSC1 and VSC2's phase angle control. [24] has further information.

B. Modified structure of UIPC

Initially, the standard UIPC's design will be altered as indicated in the preceding subsection. The next paragraph will then demonstrate the improved UIPC's control method. The standard UIPC construction, shown in fig. 3, has the following drawbacks:

Each phase employs three VSCs; as a result, nine VCSs and nine power transformers are required to link three phases of AC buses, making the architecture incredibly expensive.

All of the VSCs in each phase's DC connections are linked in parallel. Nevertheless, as stated in [12, 25], when the output voltages of the VSCs vary or when there is a disturbance in the system model, such as a change in a system parameter, the VSCs with common DC connections are disposed to the common DC link voltage oscillation. In VSCs with a shared DC link, the DC link voltage fluctuation is a significant problem. [24] does not address this problem.

The improved UIPC model, shown in Fig. 4, is suggested to eliminate the aforementioned obstacles. As shown, each phase only makes use of one power converter, known as LPC. where j is equal to one of the numbers 1, 2, or 3. Via transformers T_j, these power converters inject the series voltage $V_{se} < \varphi_{se} = V_{se}^{r} + jV_{se}^{r}$ to each line, where V_{ser} and V_{sei} are the infused series voltage's real and imaginary components, respectively. Line impedance is $Z_{Lj} = R_{Lj} + jX_{Lj}$. In most cases, the implanted series voltage is really a controlled voltage source with the general form,

$$V_{se} = K_A V_{DC} < K_p \varphi_{se} \qquad (1)$$

where KA and KP are the coefficients that determine the voltage's amplitude and phase, respectively.

The pulse width modulation (PWM) technique certainly affects the voltage amplitude coefficient (KA), the phase coefficient (KP) is 1, and the standard value of se is 2. The injection of voltage phase angle through the control system would be used to coordinate the anti-parallel thyristor switches S1 and S2. Depending on the phase angle sign, only one of these swaps at each moment. The UIPC is in inductive mode (IM), S1 is on, and S2 is off, whenever the voltage phase coefficient KP is equal to +1.

Similar to this, when S1 is off and S2 is on, the UIPC is operating in capacitive mode (CM), and the phase coefficient KP is equal to -1. Hence, management of the power exchange between the two AC buses, V1 and V2, is possible. Furthermore, note that there is just one BPC for all stages in Fig. 4. The

DC microgrid is then linked to the BPC's DC bus. To control the AC voltage and offer power exchange with the DC microgrid, the BPC is additionally linked to one of the AC buses (the weaker AC bus, i.e., the AC microgrid bus), in this case, V1, through the transformer TBPC. The system voltages' vector diagram while taking into account the injected voltage of the suggested UIPC is displayed in Fig. 5.

$$\varphi_{se}^{L} = \varphi_1 + \alpha_1$$

$$\varphi_{se}^{C} = \varphi_2 + \alpha_2 \quad \ldots\ldots \quad (2)$$

These angles are computed by taking into account the UIPC's IM or CM operating modes. When the UIPC operates in the IM and CM modes, respectively, se L and se C are the phase angles of the voltage at the middle point of the transmission line. The transferred power between the two AC buses would be calculated using the complicated power flow concept [26], which is as follows:

S= (3)

$$V_2\left(\frac{V_1-V_2}{Z_L}\right) = (V_2\cos\delta_2 + jV_2\sin\delta_2)\frac{V_1\cos\delta_1+jV_1\sin\delta_1-V_2\cos\delta_2-jV_2\sin\delta_2}{R_{L1}-jX_{L1}}$$

$$V_2\left(\frac{V_1-V_2}{Z_L}\right) = (V_2\cos\delta_2 + jV_2\sin\delta_2)\frac{V_1\cos\delta_1+jV_1\sin\delta_1-V_2\cos\delta_2-jV_2\sin\delta_2}{R_{L1}-jX_{L1}}$$

S= (4)

where $\delta 1$and $\delta 2$ are the phase angles of the voltages 1 and 2, respectively. Equation (4) may be expressed as follows after some mathematical adjustments:

$$P = \frac{R_{L1}V_1V_2(\cos\delta_1\cos\delta_2+\sin\delta_1\sin\delta_2+R_{L1}V_2^2)-X_{L1}V_1V_2(\cos\delta_1\sin\delta_2-\sin\delta_1\cos\delta_2)}{R_{L1}^2+X_{L1}^2} \quad \ldots\ldots \quad (5)$$

$$Q = \frac{R_{L1}V_1V_2(\cos\delta_1\sin\delta_2-\sin\delta_1\cos\delta_2)-X_{L1}V_1V_2(\cos\delta_1\cos\delta_2-\sin\delta_1\sin\delta_2)+X_{L1}V_2^2}{R_{L1}^2+X_{L1}^2} \quad (6)$$

In microgrids, $RL1 \gg XL1$ and we get:

$$P = \frac{V_1V_2(\cos\delta_1\cos\delta_2+\sin\delta_1\sin\delta_2+R_{L1}V_2^2)}{R_{L1}} = \frac{V_1V_2}{R_{L1}}(\cos(\delta_1-\delta_2)+R_{L1}V_2^2) \quad . (7)$$

$$Q = \frac{V_1V_2(\cos\delta_1\sin\delta_2-\sin\delta_1\cos\delta_2)}{R_{L1}} = \frac{V_1V_2}{R_{L1}}\sin(\delta_2-\delta_1) \quad \ldots\ldots \quad (8)$$

As a result, the magnitudes of the AC buses' voltages govern the transmitted active power, while the phase angle difference controls the reactive power. The proposed UIPC controls the voltage magnitude and phase angle difference, indicating that it would be simple to regulate the exchanged active and reactive powers between two AC buses. Kirchhoff Voltage Law is applied to Fig. 6 to assess the impacts of the UIPC's injected voltage, and the following results are obtained:

$$V_1 < \delta_1 - V_2 < \delta_2 = (R_{L1}+jX_{L1})I + V_{se} < \varphi_{se} = (R_{L1}+jX_{L1})\frac{P-jQ}{v_2^r-jv_2^i} + (V_{se}^r + jV_{se}^i) = \left(\frac{V_2^r(R_{L1}P+X_{L1}Q)+(X_{L1}P-R_{L1}Q)}{(v_2^r)^2+(v_2^i)^2}+V_{se}^r\right) + j\left(\frac{V_2^r(X_{L1}P-R_{L1}Q)+(R_{L1}P-X_{L1}Q)}{(v_2^r)^2+(v_2^i)^2}\right) \quad \ldots\ldots. (.9)$$

The power balance equation may be used to calculate the power that was transferred between the DC link and the AC link (V1), as shown below:

In the microgrids, $XL1P \cong RL1Q$ and we get:

$$\mathbf{V_1 < \delta_1 - V_2 < \delta_2 = \left(\frac{V_2^r(R_{L1}P+X_{L1}Q)}{(v_2^r)^2+(v_2^i)^2}+V_{se}^r\right)+jV_{se}^i} \quad (10)$$

Also, $RL1P \gg XL1Q$ and we have:

$$\mathbf{V_1 < \delta_1 - V_2 < \delta_2 = \frac{V_2^r+V_{se}^r\left((v_2^r)^2+(v_2^i)^2\right)}{(v_2^r)^2+(v_2^i)^2}+jV_{se}^i} \quad (11)$$

$$\mathbf{V_{DC}I_{DC}^{UIPC} = \frac{3}{2}V_1^dI_1^d} \quad \ldots. \quad (12)$$

Where V1d and i1d are the d-axes voltage and current of the AC link, respectively, and IDCUIPC is the current running in the DC link of the UIPC.

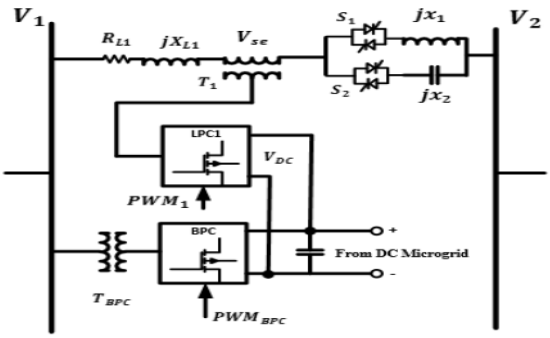

Fig.4 Proposed topology of UIPC

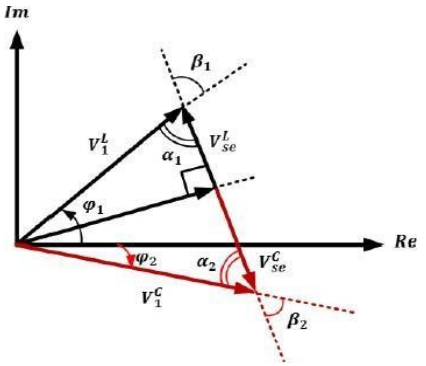

Fig.5 Voltages when the proposed UIPC is involved

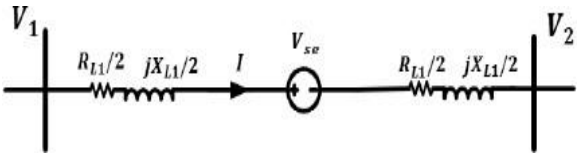

Fig. 6 Model of each phase of system considering injected voltage of UIPC

In the proposed UIPC-based interconnected microgrids for the hybrid microgrid, the per-phase architecture is depicted in Fig. 7. This graphic also displays the planned UIPC's general control structure. Series VSC control and NDO-MS-SMC-based DC link control are the two subsystems that make up the control system. An ideal H∞ based fuzzy logic controller is employed in the Series VSC Control subsystem to manage the injected voltage and switches S1 and S2, among other functions. The next paragraph gives a description of this control subsystem. The SMC-based DC link control subsystem, which is based on a new disturbance observer-based robust multiple surface sliding mode control approach, is in charge of stabilizing the common DC link voltage variations. The next section provides details on this control design process.

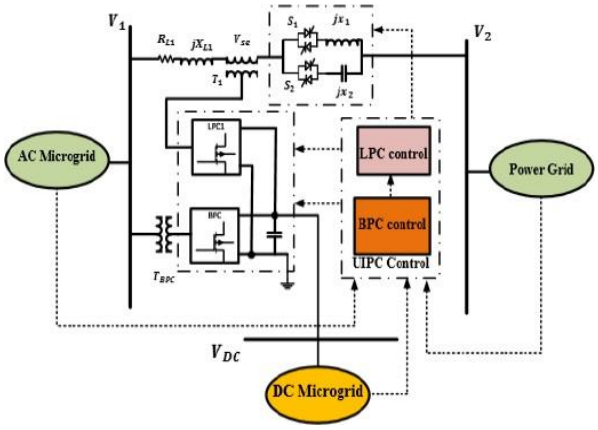

Fig. 7 Per-phase model of interconnection of AC-DC microgrids using the UIPC and control system of UIPC

Basically, the suggested UIPC topology provides the following advantages over the traditional structure:

- It simply needs one LPC per step.
- In the three-phase structure, just one BPC is necessary. Hence, the whole model requires three power transformers and four VSCs.
- The DC microgrid provides the DC link voltage.
- The UIPC can connect the AC and DC microgrids thanks to this capability.
- The control structure of the LPCs uses an ideal fuzzy logic controller, which reduces mistakes.
- A disturbance observer-based robust multiple-surface sliding mode control approach, which is detailed in the following section, is used to dampen the voltage fluctuations of the DC connection.

C. PROPOSED METHOD OF PREVENTING LPCS:

Two control subsystems—the LPC's control strategy and the SMC-based control scheme for the BPC—are included in the proposed control scheme for the proposed UIPC structure, as shown in Fig. 7. There are also control interactions between these control subsystems. The suggested control method for each LPC at each phase is shown in Fig. 8. The measured and scaled line current and injected series voltage are displayed. A bandpass filter is then used for these scaled signals in order to extract their essential components. Using MATLAB [27], the following parameters (transfer function) of this filter are established:

$$T_f = \frac{190.10s}{s^2+190.10s+145321} \quad (13)$$

The filtered signals' root means square (RMS) values are next obtained. The suggested best fuzzy logic controller is given the injected voltage error (FLC). A PLL is used to determine the voltage's injected phase. Next, depending on the sign of this phase, which is really KP in Equation (1), it is determined whether the performed, +π/2 and -π/2. Also, depending on the operating modes, switches S1 and S2 are either activated or disabled. The best FLC is created using the H filtering design procedure, which the authors of this work have fully described and validated in [8]. A DC link voltage signal is fed to the control systems of all LPCs for Synchronization, as shown in Fig. 8. An ideal FLC is then given the error signal. As a result, these signals are used to generate the control signal (reference) for implementation in the PWM unit. Equation describes how the PWM scheme is used to regulate the supplied voltage's amplitude (4.1).

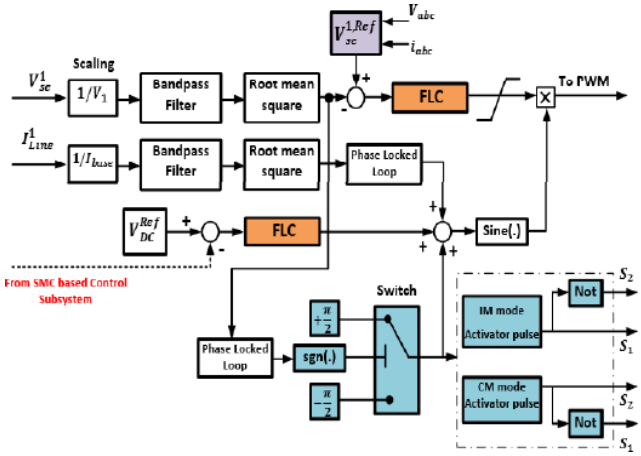

Fig.8: Control strategy for LPCs

SIMULATION RESULTS:

Based on comparative studies, simulations in MATLAB® are used in this part to assess how well the proposed power flow plan performs. The suggested improved UIPC model, as stated in Section 2, is validated in the first of four case studies. Also, the suggested strategy's regulation of the power flow between the AC microgrid and the main grid is confirmed. The power flow control from the DC microgrid to the AC microgrid is examined in the second case study, while the power flow from the AC microgrid to the DC microgrid is verified in the third. In instance 4, the stability and disturbance rejection features of the proposed UIPC are explored.

The AC microgrid consists of a 150 kW DFIG-based wind turbine system and four 50 kW diesel generators, whose datasheets may be found in [31]. The DC microgrid includes a PV system, a battery, and AC and DC loads. The ratings for the PV system and battery in this study are 250 kW and 50 kW, respectively. These data were derived from [32]. The switching gains s, Q, and P are all positive arbitrary matrices in this study, and the linear gain l2 is set to 0.7 and 0.7, respectively. As a result, the following restriction is set to 1.2, and the system starting condition to construct the suggested observer has been set to zero. Furthermore, was set to 0.001.

A. UIPC MODEL VALIDATION, AS WELL AS CONTROL OF POWER FLOW BETWEEN THE AC MICROGRID AND THE MAIN GRID

To confirm the suggested structure and further demonstrate its superiority over the conventional topology, the proposed UIPC topology, shown in Fig. 4, is compared to the traditional UIPC, shown in Fig. 3. The UIPC's parameters are therefore the same as those listed in [24]. The AC microgrid is linked to the main grid by a 2 km distribution line with a sinusoidal impedance of R_L =0.01Ω, X_L = 5mH per Phase. Analyses are done on the power flow between the microgrid and the main grid. Initially, the traditional UIPC is used to regulate how much power is sent between them. In Figs. 10–12, the simulation results are displayed. Figs. 10–13 show the reactions of the control systems.

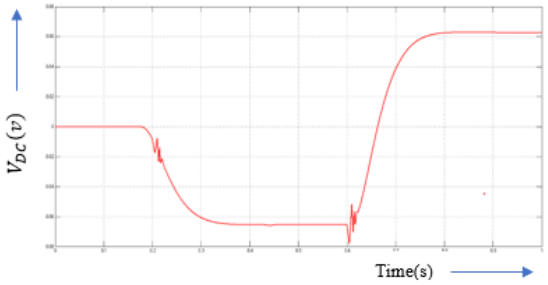

Fig.10 (a) Reference signal tracking performance of proposed UIPC equipped with new control scheme with fuzzy

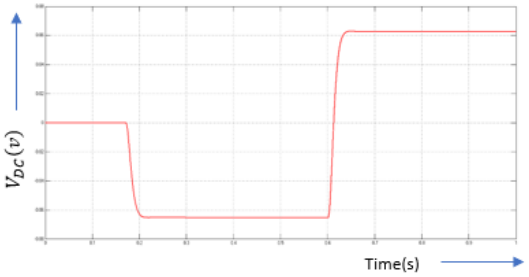

Fig.10 (b) Reference signal tracking performance of proposed UIPC equipped with new control scheme with ANFIS

In contrast to the standard UIPC structure and its control approach established in [24], shown in Fig. 10, the suggested UIPC is shown in Fig. 11 to be able to suitably follow the reference signal produced by the proposed control system. These data demonstrate how the suggested control technique acts more leniently for actual power system.

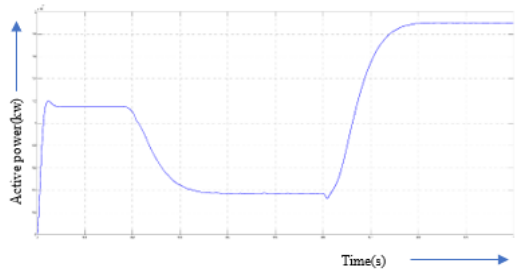

Fig.11 (a) Exchanged power (absolute value) control between two AC microgrids using proposed and conventional UIPCs using fuzzy

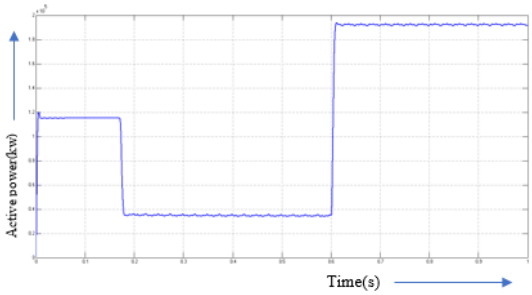

Fig.11 (b) Exchanged power (absolute value) control between two AC microgrids using proposed and conventional UIPCs using ANFIS

Fig. 11, depicts the UIPC and the proposed UIPC's exchanged power control performance. Since the UIPC is initially disabled and the system is in a steady state, no series voltage is introduced. There are 165 kW of AC and DC loads linked to the common AC bus in the AC microgrid, which only has one of the diesel generator units active. Wind turbine is initially turned off as well. The DC microgrid does not need to import power since 300 kW of total loads (which is equal to the total PV generation and ESS power) are connected to its common DC bus. Here, the AC microgrid is viewed as a fragile system. As a result, this microgrid is connected to the AC side of the BPC. Until t = 0.2s, when one of the diesel units is enabled, the AC microgrid receives 115 kW from the main power grid, as illustrated in Fig. As a result, the UIPC switches to an inductive mode and injects 0.065 PU of series voltage into the distribution line. According to Fig. 11, the swapped power is consequently reduced to about 65 kW and remains at this level until t = 0.6s, when the other diesel units and the wind turbine are turned on. In order to convert to the capacitive mode and inject 0.063pu series voltage into the distribution line, the UIPC does so. As a result, the exchanged power (absolute value) increases to 185 kW and is then provided to the main grid.

B. DC MICROGRID TO AC MICROGRID POWER FLOW CONTROL

In order to confirm the effectiveness of the suggested UIPC, the power flow performance from the DC microgrid to the AC microgrid is examined. One of the primary characteristics of the proposed structure is that the DC link of the proposed UIPC is connected to the DC microgrid, as shown in Fig. 5. The suggested NDOMS-SMC technique shown in Fig. 9 is then used to regulate the DC link of the BPC. For a scenario where the power flow is from the DC microgrid to the AC side, the simulation results are displayed in Figs. 13–14.

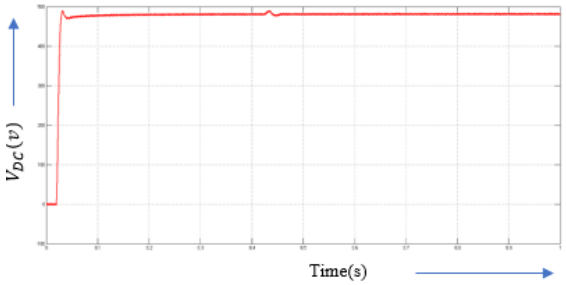

Fig.12 (a) DC link voltage when 40kw is demanded from the AC side using fuzzy

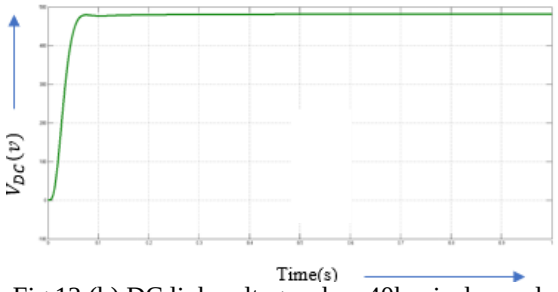

Fig.12 (b) DC link voltage when 40kw is demanded from the AC side using ANFIS

In order to keep the power transferred between the AC microgrid and main grid constant, as shown in Fig. 6.8, the AC microgrid needs 40 kW at time t = 0.42 s. The DC microgrid's internal usage is 240 kW. In order to provide the AC side, the DC link's active power rises to 280 kW, as shown in Fig. 6.7. Fig. 6.6 shows the DC link voltage in this situation. It is clear that the suggested NDO-MS-SMC approach may solve the issue of voltage fluctuations.

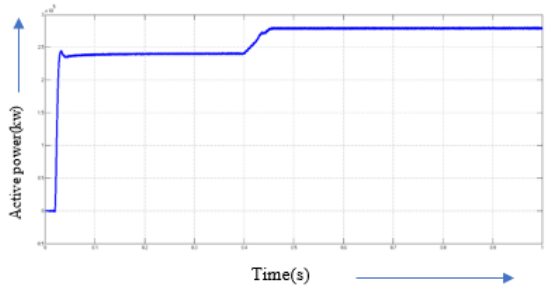

Fig.13 (a) Active power of DC link when 40kW is demanded from the AC side using fuzzy

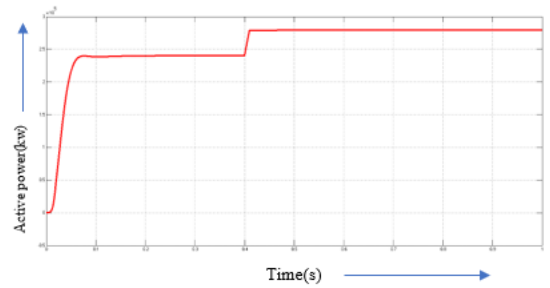

Fig.13(b) Active power of DC link when 40kW is demanded from the AC side using ANFIS

C. AC MICROGRID TO DC MICROGRID POWER FLOW CONTROL

When the power flow direction is from the AC microgrid to the DC microgrid, the simulation result is shown in Fig. 6.11. The typical AC bus power is shown in this figure. The AC microgrid initially serves 240 kW of local loads, as shown, until t = 0.42 s, when a 40kW demand is made from the DC side. As a result, the AC-side power reaches 280 kW after a reaction time of roughly 0.023 s. It has been shown that the suggested UIPC and control mechanism can softly regulate the power traded between the AC and DC microgrids.

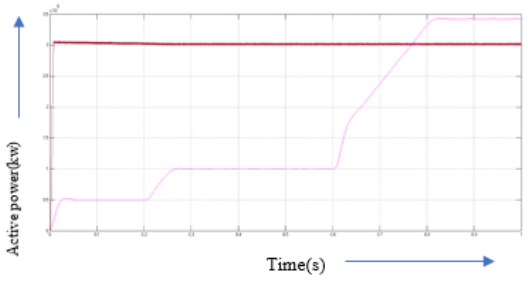

Fig.14 (a) Generation in each Microgrid using fuzzy

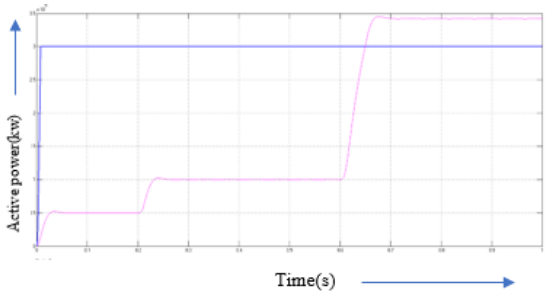

Fig.14 (b) Generation in each Microgrid using ANFIS

The generation in each microgrid is depicted in Fig. 6.8. As shown in Fig. 6.5, the proposed UIPC and its control technique are able to smoothly transfer power between the hybrid microgrid and utility, in contrast to the standard UIPC structure, which exhibits oscillatory behavior due to its excessive parallel connection of power converters. According to Fig. 6.5, the suggested UIPC settles in less than 2 seconds, which is more than 50% quicker than the standard UIPC, which takes around 4 seconds to do so. When the traditional UIPC is executed, there is an overshoot of about 37.14%; however, there is no overshoot when the suggested UIPC is applied.

d. Disturbances are rejected as proof of performance and stability

The time-varying signal is regarded as a disturbance in the system model to test its robust stability and disturbance rejection capabilities. IL, or the lumped DC load current, is the disturbance. Additionally, adjustments of 10% are made to the AC side voltage. In such cases, the key worry is the stability of the UIPC's DC connection. The outcomes of the simulations for the suggested UIPC and the traditional UIPC. As shown, the conventional UIPC brings many oscillations with very high transients, whereas the proposed UIPC integrated with the new control mechanism has better performance and keeps the system stable as well.

CONCLUSION

Future smart grids are most likely to use hybrid microgrid structures to combine AC/DC demands with renewable energy sources. This is because this construction simultaneously benefits from both AC and DC microgrids. The power exchange regulation between linked AC and DC microgrids is a typical issue with this layout. A UIPC-based strategy has been presented in this study as a preferable replacement for the parallel-connected power converters, which have caused several issues. Effective control measures have

subsequently been developed for the updated UIPC after a new structure for the UIPC was first proposed. The enhanced UIPC based on the ANFIS controller and sliding mode controller is the subject of this article. performance of power exchange management between AC and DC micro-grids. This method was created to address a variety of shortcomings and issues with the ANFIS controller. The improved model and the power exchange control performance between AC and DC microgrids were both proven by the simulation results.

REFERENCES

[1]. Jia Lihu, et al, "Architecture Design for New AC-DC Hybrid Microgrid", DC Microgrids (ICDCM), IEEE First International Conference on, 2015.

[2]. Akanksha Mishra and G.V. Nagesh Kumar, "Congestion Management of Power System with Interline Power Flow Controller Using Disparity Line Utilization Factor and Multi-objective Differential Evolution" CSEE Journal of Power and Energy Systems, Volume: 1, Issue: 3, pp. 76 - 852015.

[3]. B. Vijay Kumar, et al., "Optimization of UPFC location and capacity to improve the stability using ABC and GSA algorithm", IEEE, Power and Energy Conference at Illinois (PECI), 2015.

[4]. Suzan Eren, et al., "An Adaptive Droop DC-Bus Voltage Controller for a Grid-Connected Voltage Source Inverter with LCL Filter", IEEE Transactions on Power Electronics, Volume: 30, Issue: 2, pp.547 – 560, 2015.

[5]. Mahdig Zolfaghari, et al, "A Fractional Order Proportional-Integral Controller Design to Improve Load Sharing between DGs in Microgrid", Smart Grids Conference (SGC), 20-21 Dec. 2016, Graduate University of Advanced Technology, Kerman, Iran, 2016.

[6]. [6] Huanhai Xin, et al., "A Decentralized Hierarchical Control Structure and Self-Optimizing Control Strategy for F-P Type DGs in Islanded Microgrids", IEEE Transactions on Smart Grid, Volume: 7, Issue: 1, pp. 3 – 5, 2016.

[7]. The MathWorks, Inc., MATLAB Software, version 9.1.0, 2016.

[8]. Pengcheng Yang, et al, "A Decentralized Coordination Control Method for Parallel Bidirectional Power Converters in a Hybrid AC/DC Microgrid", IEEE Transactions on Industrial Electronics, EarlyAccess, 2017.

[9]. Ignacio Gonzalez-Prieto, et al, "Impact of Postfault Flux Adaptation on Six-Phase Induction Motor Drives with Parallel Converters", IEEE Transactions on Power Electronics, Volume: 32, Issue: 1, pp.515 – 528, 2017.

[10]. S. A Taher, M. Zolfaghari, C. Cho, M. Abedi, M. Shahidehpour, "A New Approach for Soft Synchronization of Microgrid Using Robust Control Theory", IEEE Transactions on Power Delivery Volume: 32, Issue: 3, pp. 1370 – 1381, 2017.

[11]. Daniel K. Molzahn, et al, "A Survey of Distributed Optimization and Control Algorithms for Electric Power Systems", IEEE Transactions on Smart Grid, Early Access, 2018.

[12]. Cuo Zhang, et al, "Robustly Coordinated Operation of a Multi-Energy Microgrid with Flexible Electric and Thermal Loads", IEEE Transactions on Smart Grid, Early Access, 2018.

[13]. Samrat Acharya, et al, "A Control Strategy for Voltage Unbalance Mitigation in an Islanded Microgrid Considering Demand Side Management Capability", IEEE Transactions on Smart Grid, Early Access, 2018.

[14]. Mahdi Zolfaghari, et al, "A New Power Management Scheme for Parallel-Connected PV Systems in Microgrids", IEEE Transactions on Sustainable Energy, Early access, 2018.

[15]. Runfan Zhang, Branislav Hredzak, "Distributed Finite-Time Multi-Agent Control for DC Microgrids with Time Delays", IEEE Transactions on Smart Grid, Early Access, 2018.

[16]. Kumar Utkarsh, et al, "Distributed Model-predictive Real-time Optimal Operation of a Network of Smart Microgrids", IEEE Transactions on Smart Grid, Early Access, 2018.

[17]. Jongwoo Choi, et al, "Robust Control of a Microgrid Energy Storage System using Various Approaches", IEEE Transactions on Smart Grid, Early Access, 2018.

[18]. Mahdi Zolfaghari, Student Member, IEEE, Mehardad Abedi, Member, IEEE, Gevork B. Gharepetian, Senior Member, IEEE.